BOLLETTINO DI GEOFISICA TEORICA ED APPLICATA VOL. XXXIV, N. 134-135 - JUNE-SEPTEMBER 1992

E. BRIZZOLARI[1], L. ORLANDO[1], S. PIRO[2] and L. VERSINO[2]

GROUND PROBING RADAR SURVEY IN SELINUNTE ARCHAEOLOGICAL PARK

Abstract. This paper describes the results obtained from a survey with Ground Probing Radar on the Eastern Hill of the Archaeological Park of Selinunte (Sicily, Italy). Two different test sites were surveyed: a northern area with probable Roman remains (40×40 area) and a southern one with probable Precolonial habitations (90×90 area). In the first area, the interpretation of the data collected shows good agreement with the results obtained from magnetic surveys. In the second, the results show the irregular surface shape of the upper part of a calcarenitic layer under the soil.

INTRODUCTION

This paper describes the results obtained with the G.P.R. (Ground probing radar) method in two sample areas (40×40 m and 90×90 m) on the Eastern Hill and near Temple G in the Selinunte Archeological Park (Fig. 1).

As archeological structures are formed by bodies of limited extent at shallow depth, the associated anomalies are generally small and may be masked by various disturbances. Moreover, the anomalous bodies may be of the same material as the enclosing soil. Such bodies can sometimes be identified by the surface enclosing them, if a small volume of the material forming the contact has different physical properties. One of the techniques useful in a situation like this is the G.P.R. method.

Ground probing radar has become increasingly popular in civil engineering and archeological investigations in the last few years (Bevan et al., 1975; Weymouth, 1986; Tsuneo et al., 1987; Bevan, 1991) as a tool for detecting underground discontinuities, such as buried pipes, brick walls, cavities, stratigraphic contact surfaces, etc. (Annan et al., 1976; Ulriksen, 1983; Finzi et al., 1991).

Because the area investigated is wide, the measurements were taken only in an anomalous zone, as indicated by other methods (Brizzolari et al., 1992a, 1992b). Moreover, GPR is one of the less time consuming geophysical methods.

Archeologists describe the Eastern Hill zones of the Selinunte Park as a possible Precolonial human settlement to the north of the Temples, and as a Roman settlement in the northern portion of the Hill. The Precolonial settlement would be formed of buildings arranged according to a regular pattern with foundations laid in geometrically simple rock excavations (squares or rectangles). The presumed Roman structures are remains of walls, pavements and hearth stones.

Manuscript received January 15, 1992; accepted March 18, 1992.

[1] Dipartimento Idraulica Trasporti e Strade, Area Geofisica, Univ. La Sapienza, via Eudossiana 18, 00184 Roma, Italy.

[2] Istituto per le Tecnologie Applicate ai Beni Culturali - C.N.R., P.O. Box 10, 00016 Monterotondo Staz. (Roma), Italy.

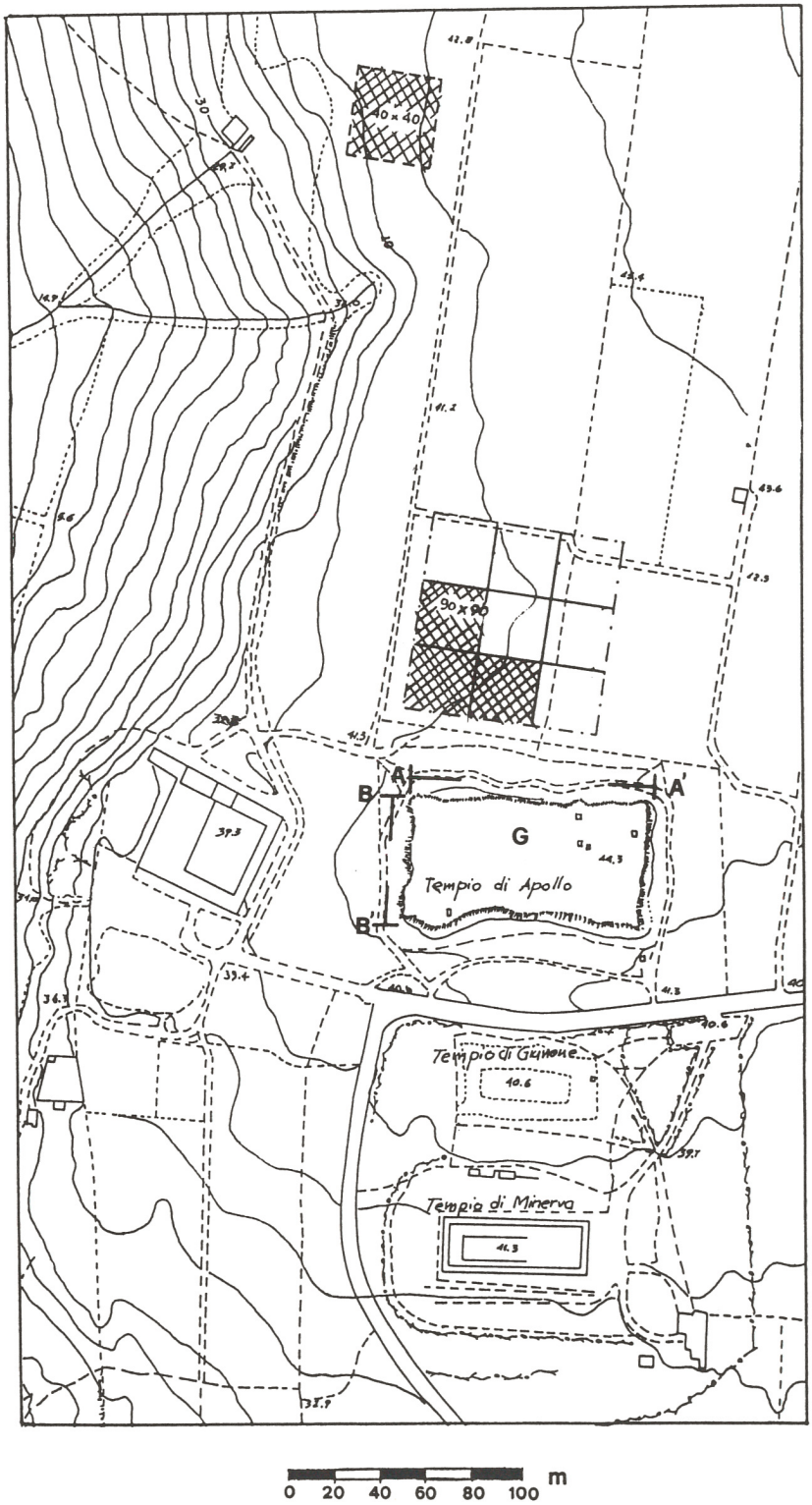

Fig. 1 — Map of the Eastern Hill. Location of Ground probing radar survey. AA, BB: radar profiles near Temple G.

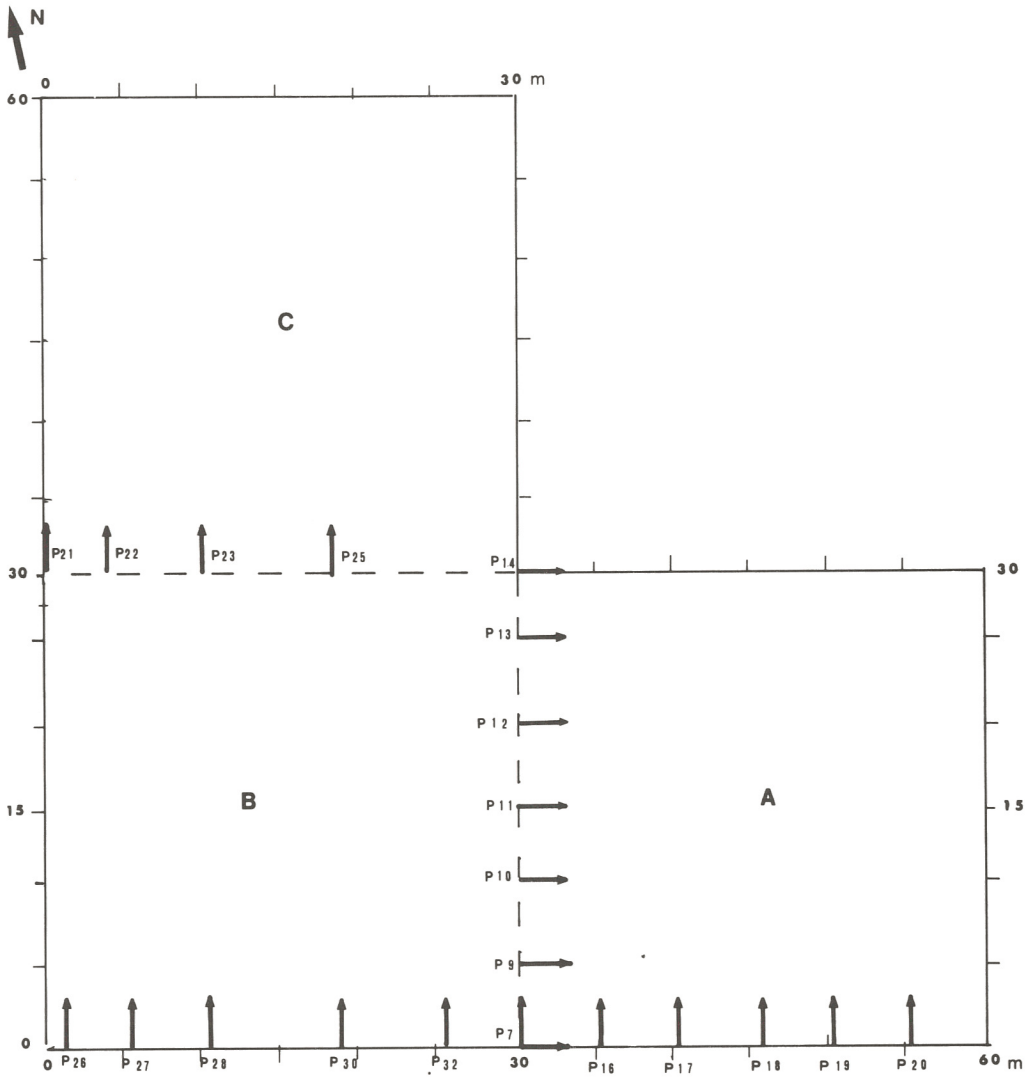

Fig. 2 — 90×90 area. Position of radar profiles in the three squares a), b), and c.

DATA COLLECTION

The two sample areas on the Eastern Hill are conventionally called the "40×40" (Roman settlement) and "90×90" (Precolonial settlement). The survey was carried out with a Georadar YL R2, mod. 2441 from OYO using 600 MHz antennas. At the beginning, both transmitter and receiver were located near each other in order to reduce the noise produced by direct waves in the ground. Unfortunately, this configuration caused great antenna interference throughout the records. Therefore, it was necessary to separate the antennas to obtain a compromise between the influence of direct waves and interference of antennas. Good results were obtained with a distance of 100 cm.

The signal propagation rate (7 ÷ 11 cm/ns) was measured with a series of WARR (Wide-Angle Refraction and Reflection method) profiles.

The various stages of data acquisition are described hereafter separately for each area.

The "40×40" area

From the geomorphological point of view, the area is characterised by flat morphology with a gentle westwards slope. The soil has a clayey matrix and includes fragments of rocks and artifacts (bricks and ceramics). Its thickness is about 50 cm, and it covers a sand-clay formation. During the survey (May 1990), the soil was particularly dry, a situation favouring signal penetration.

After a few initial signal calibration tests based on site geoenvironmental features and the supposed target (i.e., remains of wall and pavements), the following instrument configuration was chosen: i) time scale t=100 ns; ii) passband filters: HPF-LPF 20÷800 Hz.

This configuration was used for two series of radar scans: one of fifteen 40-m long parallel profiles stretching E-W and numbered from P1 to P15; the other series was oriented perpendicularly to serve as a check, and consisted of eight 40-m long N-S trending parallel profiles numbered T1 to T8.

Each profile has markers every two meters. The interval between adjacent profiles was kept constant except when obstacles were encountered. Data were recorded analogically on a graphic recorder and on magnetic tapes.

The "90×90" area

The "90×90" area also has a flat morphology, but lithology is different: below a thin (30÷50 cm) clayey soil with fragments of calcarenitic rock and gravel, there is a thin calcarenitic layer that is probably weathered and fractured, as mentioned elsewhere in this issue (Amadori et al.; Brizzolari et al., 1992b). Profiles in this area were taken in 3 of the 9 squares (30×30) (see Fig. 1) displaying various magnetic anomalies. As shown elsewhere (Brizzolari et al., 1992b), there is a SW-NE linear anomaly in the southwestern square, and other small anomalies are spread over the southern part of the area.

From the results of calibration tests, the following instrument configuration was adopted: i) time scale: t=100 ns; ii) passband filters: HPF-LPF=160÷800 Hz, which was used to carry out the following radar scans (Fig. 2): square (a), seven equidistant parallel profiles in the W-E direction, and 6 N-S trending profiles perpendicular to them; square (b), five N-S trending parallel profiles; square (c), four N-S trending parallel profiles. All the profiles are 30 m long with a marker every 2 metres.

Profiles near temple G

Other two profiles were taken parallel to the northern and western sides of Temple G (Fig. 1). These profiles (120 m long with a marker every 2 m, and instrumental configuration: i) time scale: t=100 ns; ii) passband filters: HPF-LPF=40-400 Hz) were taken in order to identify possible anomalies linked to the temple structure.

Although the distance from the 90×90 area is less than 20 m, the lithology is quite different. As reconstructed by vertical electric soundings (Brizzolari et al., 1992b), the Temples zone is characterized by a compact layer of calcarenite many meters thick with resistivity higher than 1000 Ωxm. The geological survey (Amadori et al., 1992) postulates a fault with E-W direction near Temple G.

DATA INTERPRETATION

The prospecting instrumentation used, as above mentioned, was able to provide analogic recording of data by means of both graphic and tape recorders. Because digital data recording was not available, it was impossible to process data to improve definition and the signal/noise ratio. Notwithstanding, the quality of the analogic records is such as to be useful for the scope of the research.

If the results of the WARR profiles are taken into account (velocity range 7÷11 cm/ns see above) and if the length of the reflected impulses is estimated as 5 ns, the vertical resolution

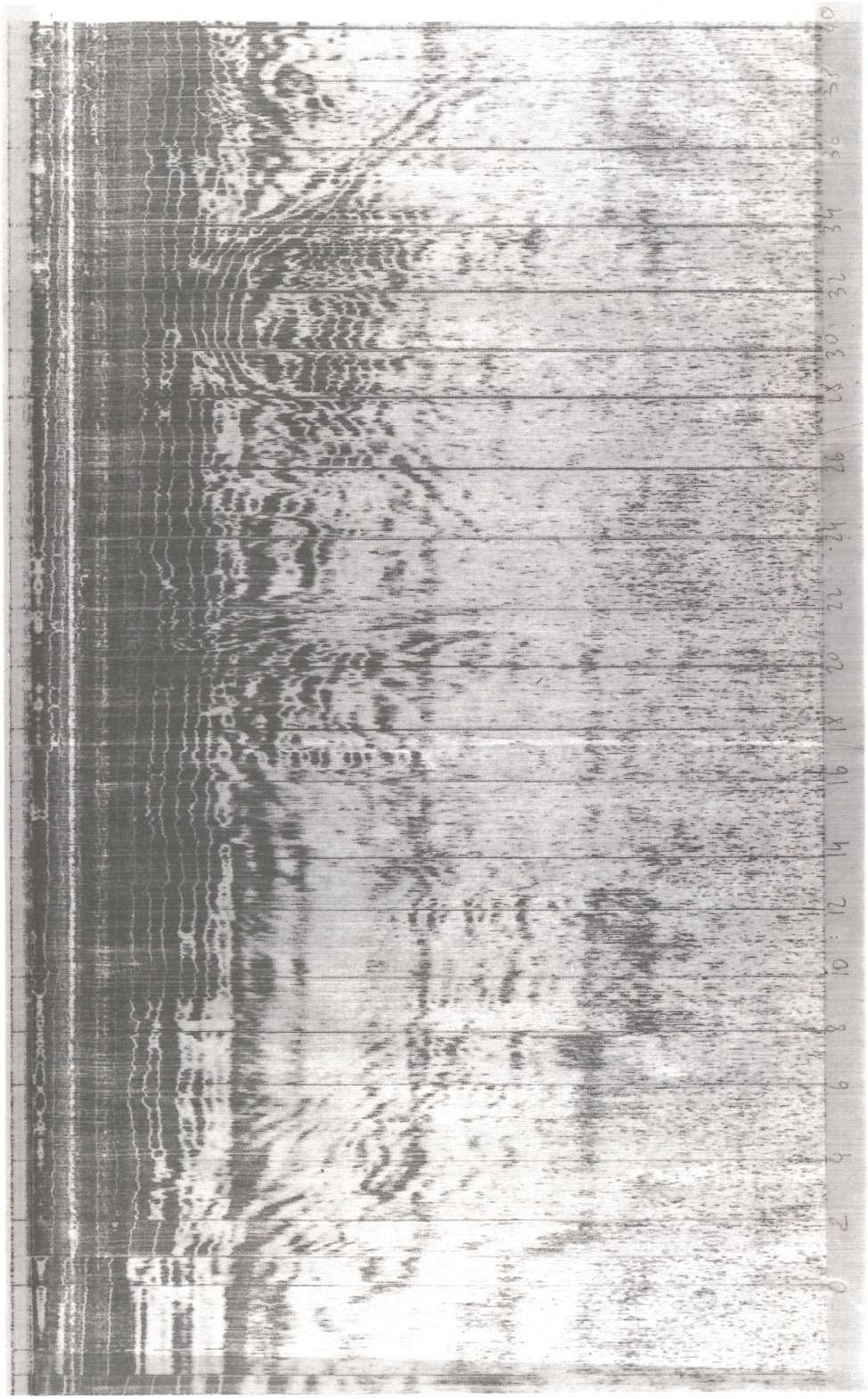

Fig. 3 — 40×40 area. Example of radar recording with type A anomaly.

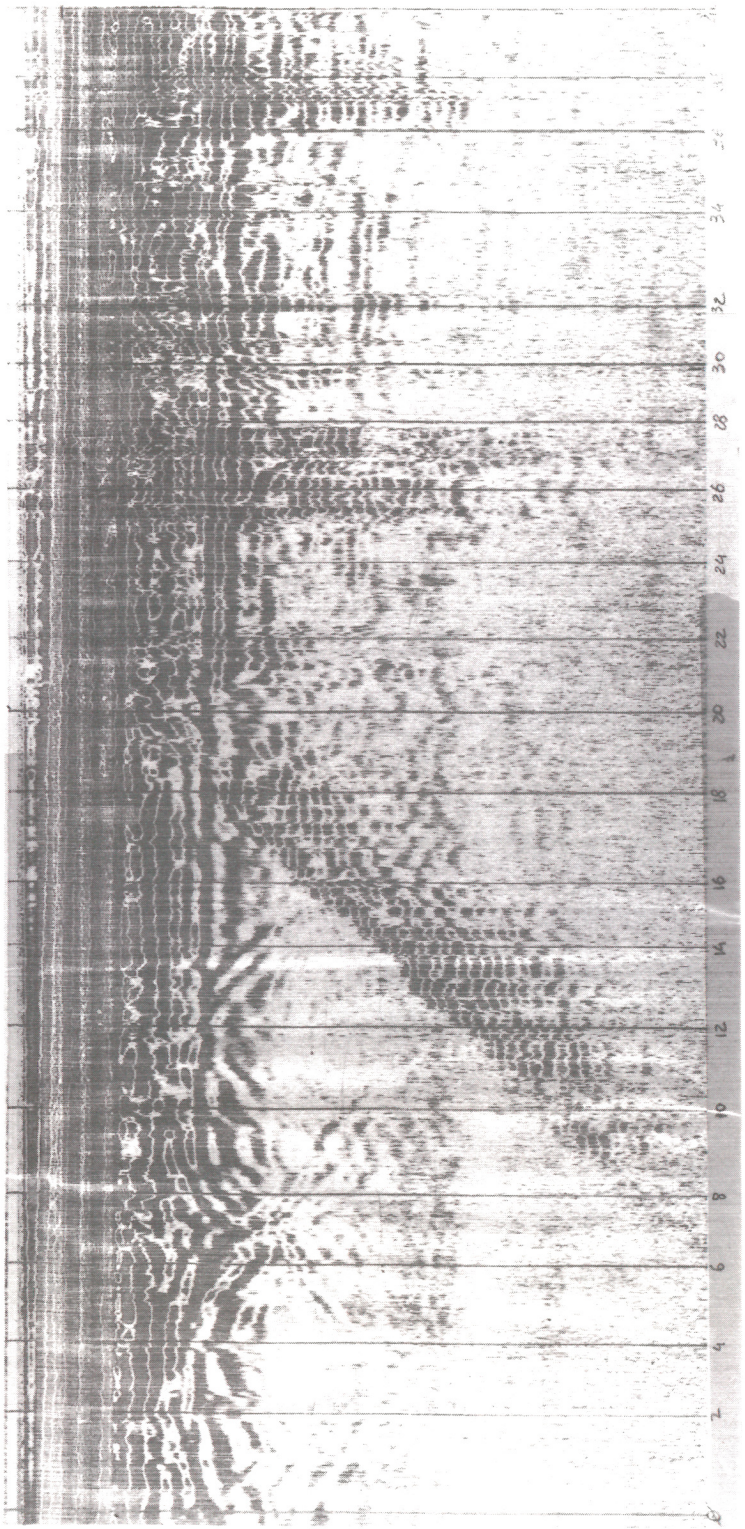

Fig. 4 — 40×40 area. Example of radar recording with types B and C anomalies.

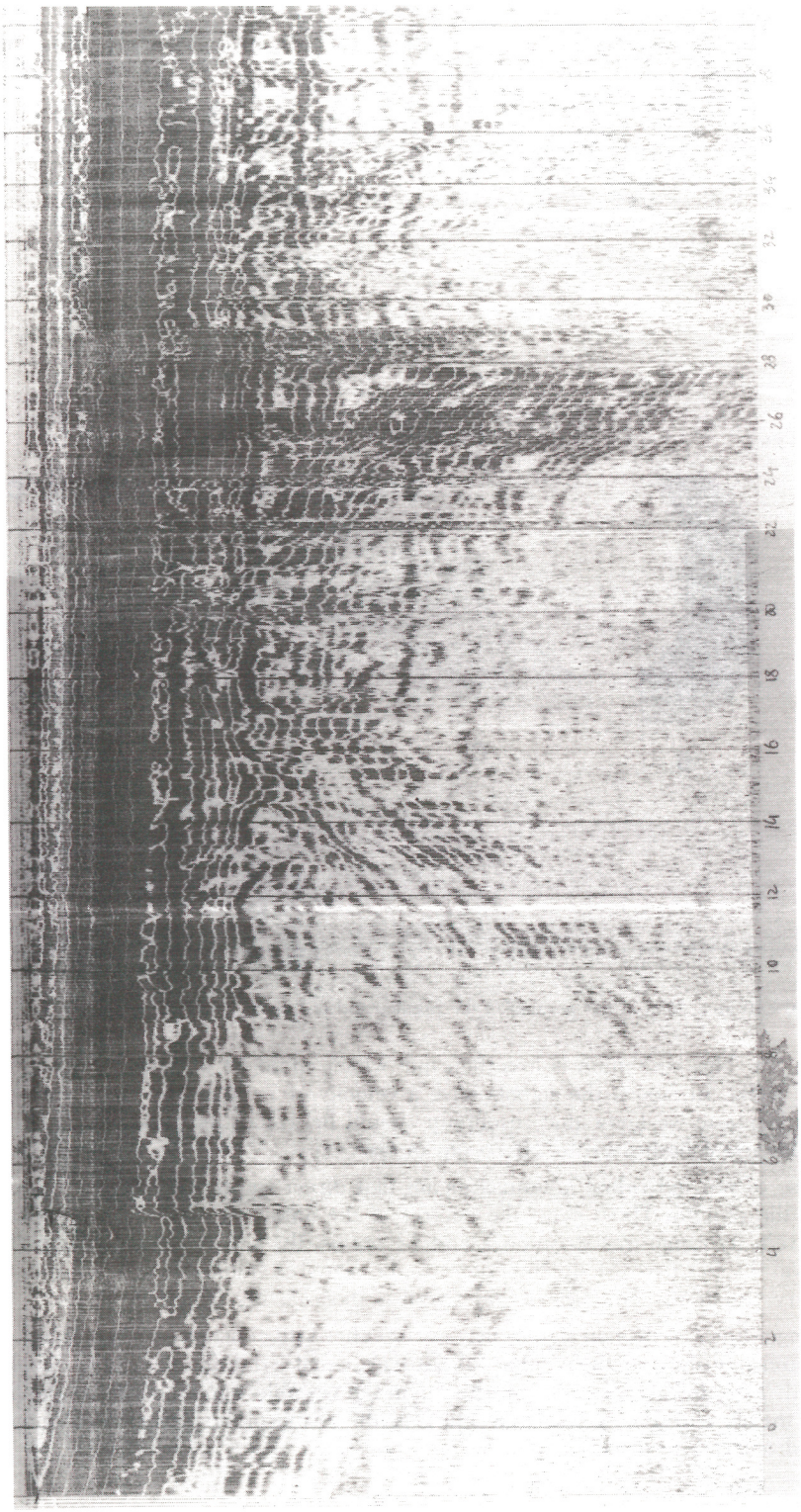

Fig. 5 — 40×40 area. Example of radar recording with type D anomaly.

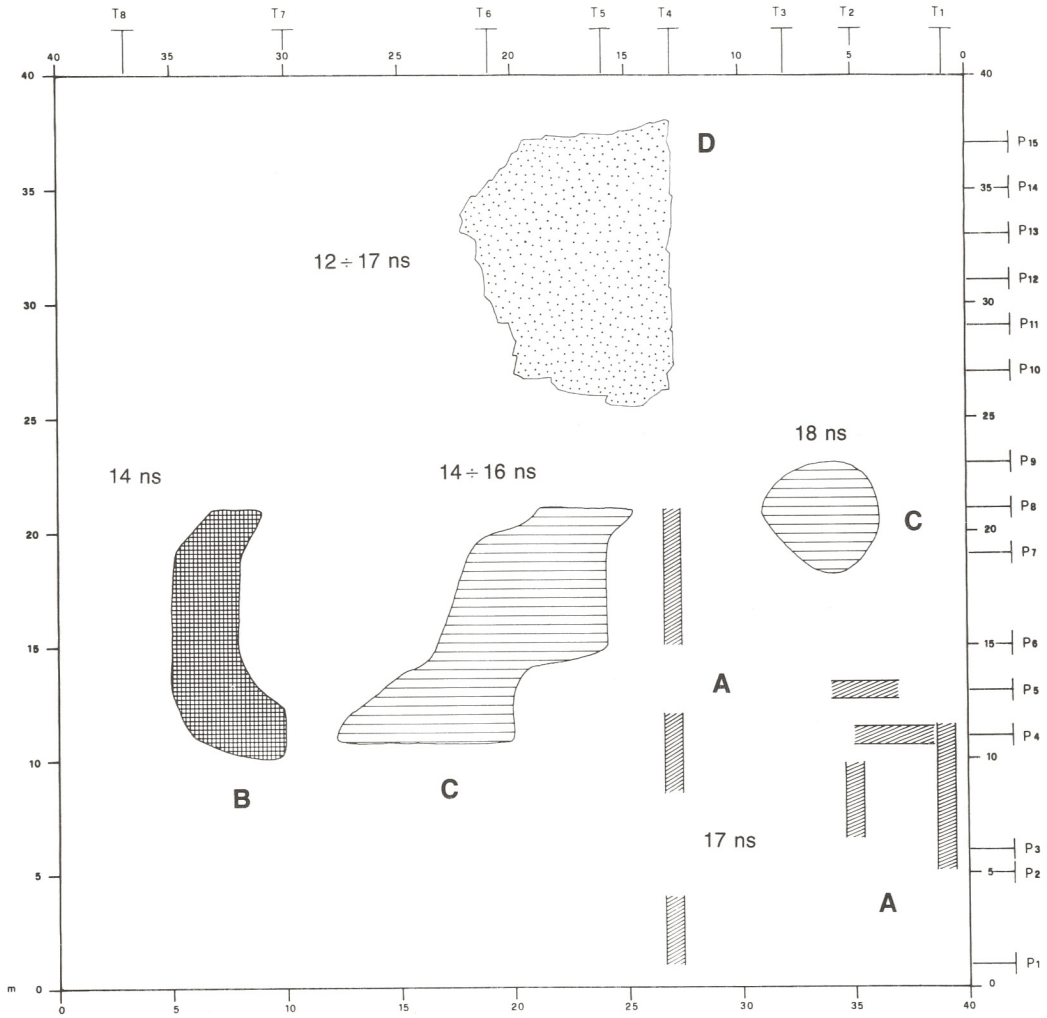

Fig. 6 — 40×40 area. Map of the position of the profiles and of different types of anomalies.

is 35 ÷ 55 cm. This resolution is less than that which could be obtained with the frequency used (600 MHz). In fact, if the signals have a velocity of 7-11 cm/ns, their wavelengths are 42-66 cm. Because we know that resolution should be 1/4 of the wavelength, the antennas used should reveal bodies up to 10-16 cm in size.

The use of two individual antennas meant that direct waves were the first arrival in the air and in the ground. Thus, since the centres of the antennas were 100 cm apart and the estimated velocity range was between 7 and 11 cm/ns, the records have a blind zone in the time interval 0 ÷ 9/14 ns twt. In this interval, the signal is homogeneous, saturated and has no geometry variations. Thus the useful signal is that starting from 9 ÷ 14 ns.

For longer times, reflection signals may occur either with constant or very variable character over wide areas. In studying the results of the survey, a marked difference in the signal character was noticed. Therefore, taking into consideration the variable signal character, the lithological features of the areas and the archeological targets, the results of the prospections in the different areas are discussed separately.

The "40×40" area

Anomalies in this area are mostly located between 12 and 20 ns twt with very different

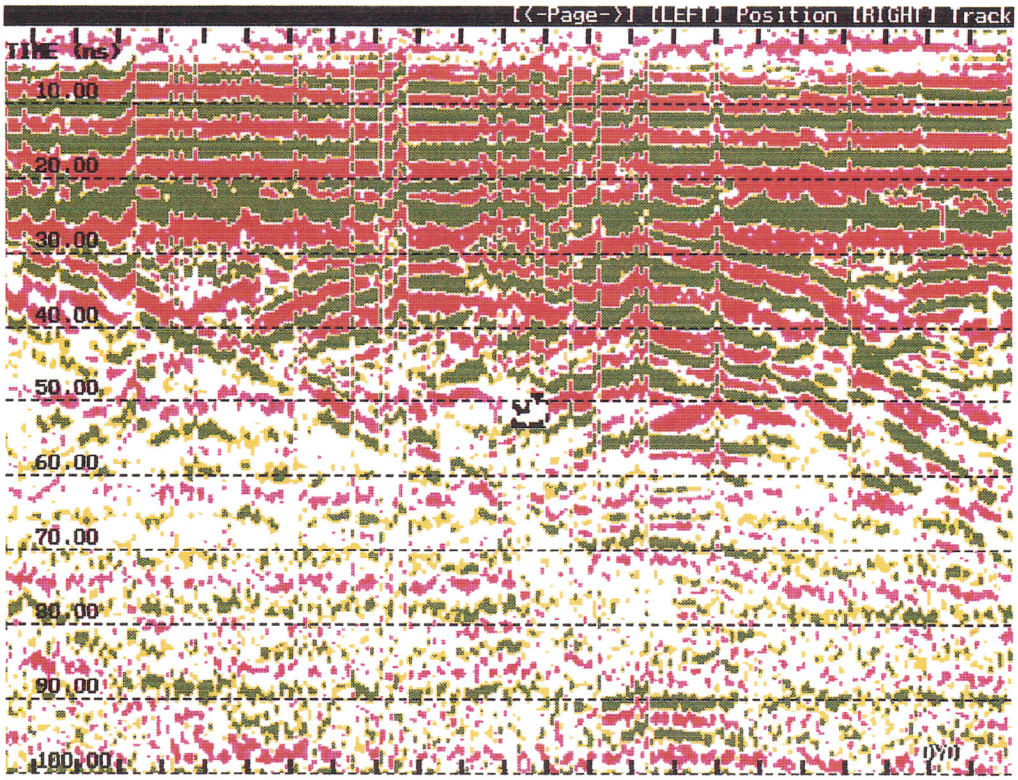

Fig. 7 — 90×90 area. Example of radar recording.

reflection signatures from zone to zone. Thus, the anomalies have been grouped into 4 types.

Type A anomalies (an example of which is shown in Fig. 3) are characterized by a strong signal and are continuous over distances of up to 3 ÷ 4 m. The reflections can be detected at the depth of 16 ÷ 18 ns twt and display diffraction hyperbolas at the borders.

Type B anomalies (Fig. 4) consist of a discontinuous signal of small amplitude with variable lateral characteristics than Type A anomalies. Occasional ringing may continue for many nanoseconds. Figure 4 shows an example of this type of anomaly, which is followed uninteruptedly eastwards by a reflecting surface (C) inclined at 12-18 degrees, assuming the propagation rate of the electromagnetic waves in the ground is 7-11 cm/ns, respectively.

The signal from this surface is very clear, of small amplitude and is associated with evident ringing. This anomaly (C) has been identified in sections P4-P5-P6.

A fourth type of anomaly (D) is not clearly visible and can best be discerned from the diffraction hyperbolas accompanying it (Fig. 5).

All the types of anomalies are shown in the map of Fig. 6 with different symbols.

Because the responses of the signals from the various reflecting surfaces vary greatly from one surface to another, it is assumed that the anomalies in the area are caused by reflecting surfaces with different geometric and/or electromagnetic features.

The absence of correlated reflections below 50 ÷ 60 ns, unless due to absorbtion phenomena, suggests that there is a single horizon up to the depth of 3.5 ÷ 5.5 m (100 ns twt) in the zone.

The "90×90" area

An analysis of the profiles obtained in the zone shows reflections with similar electromagnetic characteristics over the entire area. The signal is of high intensity at 25 ns twt and continues

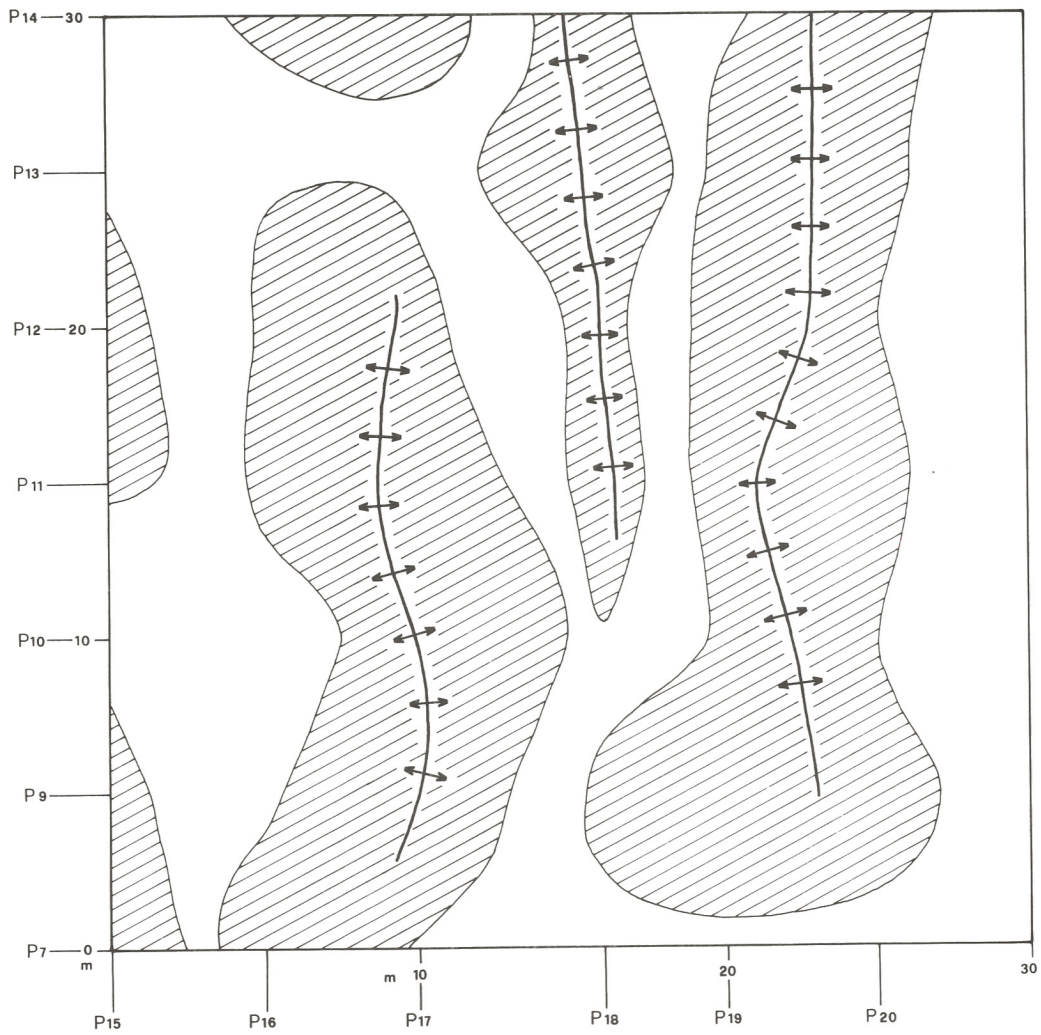

Fig. 8 — 90×90 area. Square a). Map of the individuated anomalies and their longitudinal axis.

for a few nanoseconds. In some cases, it is possible to discriminate discordances inside the reflections; this suggests that there is more than one reflecting surface below the instrument's vertical resolution because of the wave train length (5 ns). It is worth noting that the signal is more homogeneous in the E-W direction than N-S.

The reflecting surface is more continuous near Temple G (Fig. 7), while, futher north, the signal is frequently interrupted and feeble.

The anomalies have slightly convex surfaces, and there is a curvature hyperbolic signal at their borders. Theoretical diffraction hyperbolas, calculated for the identified depths and for a velocity of 7 ÷ 11 cm/ns, are much more inclined than those on the records; this excludes them being diffraction hyperbolas: the observed reflections are to be considered caused by real surfaces having a curvature higher than that visible in the profile, due to the migration effect. For the 30×30 sq.m area, which has been densely surveyed (Zone "a" in Fig. 2), the reflecting surfaces discriminated are shown in the map of Fig. 8 as dashed areas. Reflecting bodies are 5 to 8 m wide in the E-W direction whereas they may be more than 30 m long in the N-S direction.

Recordings carried out in the other parts of the 90×90 area display similar characteristics, but it was not possible to make a detailed reconstruction of the reflecting bodies owing to the

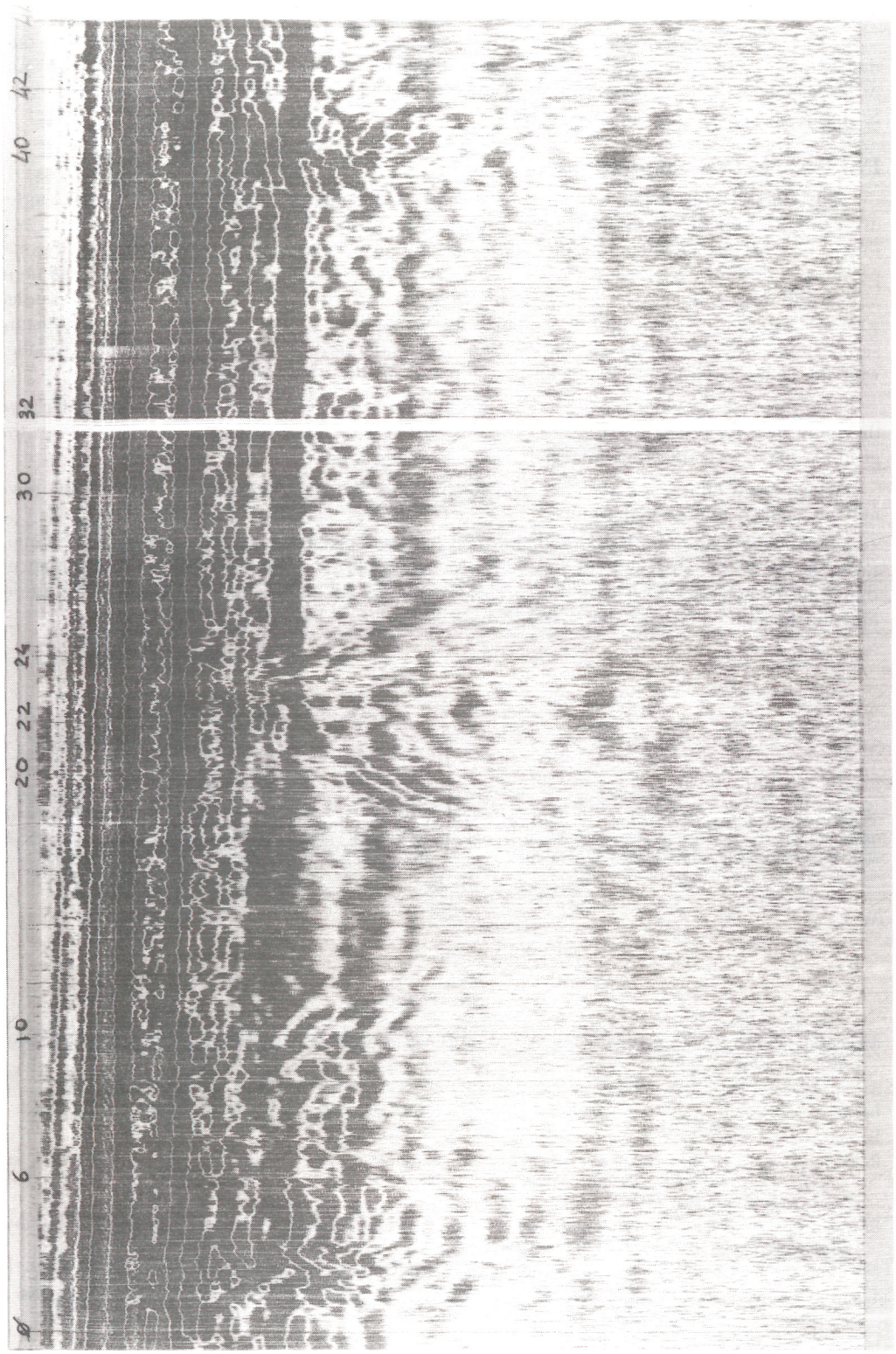

Fig. 9 — Temple G. Example of radar recordings.

small number of profiles taken.

The continuity and extent of the response of the reflecting horizon suggest that the surface defined in the 90×90 area may relate to a geological boundary. In accordance with the results of the geological survey (Amadori et al., 1992), we believe that the Georadar has been able to define the calcarenite upper surface.

Profiles near the temple G area

The Georadar profiles taken out near Temple G parallel to its northern and western sides are characterised by mainly homogeneous and subhorizontal signals. At about 25-30 ns twt, there is a very strong reflection attributable to the calcarenite upper surface. However, some portions of this surface display $2 \div 3$ m long anomalies associated with diffraction phenomena and a pull-down effects (see Fig. 9). This suggests that the anomalies are related to bodies with a velocity lower than that of the surrounding medium. Three anomalies with a constant separation of $40 \div 42$ m have been distinguished on the northern side, whereas two anomalies with the same separation have been individuated on the western side.

The interaxial regularity, the extent of the anomalies, the electromagnetic response and the pull-down effect suggest that these anomalies may be related to artificial trenches in the ground, filled with different materials to the surroundings.

Other small anomalies are also recognizable but are of dubious interpretation and have not been taken into consideration.

As a concluding remark, based mainly on previous considerations of the method's resolution numerical processing of the field data will be necessary. This will be possible with the advanced digital instrumentation already on sale. The processing will on one hand give better resolution, and on the other increase the signal to noise ratio.

Acknowledgements. The authors thank: Gianfranco Morelli for technical collaboration; Mario Mazza for the photographic documentation; Renato Caciagli, Mario Mazza and Gaetano Pappalardo for the topographic survey; and Mario Mascellani for the drawings in this work.

REFERENCES

Amadori L., Feroci M. and Versino L.; 1992: *Geological outline of the Selinunte Archaeological Park*. Boll. Geof. Teor. Appl., **34**, 00-00.

Annan A.P. and Davis J.L.; 1976: *Impulse radar soundings in permafrost*. Radio Science, **11**, 383-394.

Bevan B. and Keyon J.; 1975: *Ground probing radar for historical archaeology*. Masca Newsletter, **11**, 2-7.

Bevan B.; 1991: *The search for graves*. Geophysics, **56**, 1310-1319.

Brizzolari E., Cardarelli E., Feroci M., Orlando L., Piro S. and Versino L.; 1992a: *Vertical electric soundigs and inductive electromagnetism used to characterize the calcarenitic plate in the Selinunte archaeological Park*. Boll. Geof. Teor. Appl., **34**, 00-00.

Brizzolari E., Cardarelli E., Feroci M., Piro S. and Versino L., 1992b: *Magnetic survey in the Selinunte Archaeological Park*. Boll. Geof. Teor. Appl., **34**, 00-00.

Finzi E. e Piro S.; 1991: *Metodo per impulsi elettromagnetici: Georadar*. Quaderni dell'ITABC, C.N.R., **1**, 53-70.

Tsuneo I., Toshihiko S. and Takoshi K.; 1987: *Use of ground probing radar and resistivity surveys for archaeological investigations*. Geophysics, **52**, 137-150.

Ulriksen C.P.; 1983: *Application of impulse radar to civil engineering*. Geoph. Surv. System.

Weymouth J.W.; 1986: *Geophysical methods of Archaeology site surveying*. Advances in Archaeology method and theory, **9**, 311-395.